THREE-DIMENSIONAL SUBSATELLITE MOTION UNDER AIR DRAG AND OBLATENESS PERTURBATIONS*

J. C. VAN DER HA**

European Space Operations Centre, Darmstadt, F.R.G.

(Received 29 October, 1979; accepted 23 March, 1981)

Abstract. The three-dimensional relative motion of a subsatellite with respect to a reference station in an elliptical orbit is studied. A general theory based on the variation of the relative elements, i.e. the instantaneous differences between the orbital parameters of the subsatellite and those of the station, is formulated in order to incorporate arbitrary perturbing forces acting on both satellites. The loss of precision inherent in the subtraction of almost identical quantities is avoided by the consistent use of difference variables. In the absence of perturbations exact analytical representations can be obtained for the relative state parameters. The influences of air drag and Earth's oblateness on the relative motion trajectories are investigated and illustrated graphically for a number of cases.

List of Symbols

a	semi-major axis
$\mathbf{a}$	set of six orbital parameters, Equation (11)
c_{jm}	coefficients in expansion of C_j, Equation (22)
e	eccentricity
f, g	orbital parameters, Equations (12)
h	angular momentum per unit mass, $\lvert\mathbf{r} \times \mathbf{v}\rvert$
i	inclination
j, k	orbital parameters, Equations (12)
l	semi-latus rectum, $a(1 - e^2)$
m	mass of satellite
$\mathbf{r}$	orbital radius vector
t	time
$\mathbf{u}_j$	$(j = x, y, z)$ unit vector along local j-axis
$\mathbf{v}$	velocity vector
$\mathbf{w}$	rotation vector of local reference frame with respect to inertial space
x, y, z	local coordinate axes, Figure 1
A	cross-sectional area of satellite exposed to air flow
$A = [\alpha_{jk}]$	$(j, k = 1, 2, 3)$ rotation matrix, Equations (A1)
C	drag coefficient
C_j	Fourier coefficients of τ, Equation (21)
E	eccentric anomaly
$\mathbf{F}$	perturbing acceleration vector
G_j	$(j = x, y, z)$ auxiliary functions, Equations (18)
H	density scale height
J	auxiliary function, Equations (18)
J_2	second zonal coefficient of Earth's gravity field, 1.0827×10^{-3}
L	true longitude

* Paper presented at the 30th congress of the International Astronautical Federation, Munich, W. Germany, Sept. 16–22, 1979, Paper No. IAF 79–188.

** Aerospace Engineer.

Celestial Mechanics **26** (1982) 285–309. 0008–8714/82/0263–0285 $03.75.

M	mean anomaly
R	range between probe and station
R_e	Earth's equatorial radius, 6378.2 km
T_∞	exospheric temperature
$\mathbf{U}_j$	$(j = 1, 2, 3)$ unit vector along inertial X_j-axis
V	disturbing potential due to Earth's oblateness
$\mathbf{V}$	abbreviation for $\mathbf{w} \times \mathbf{x}$
X_1, X_2, X_3	inertial coordinate axes, Figure 1a
α, β	cone and clock angles of probe's position relative to station, Figure 1b
α_{jk}	$(j, k = 1, 2, 3)$ elements of rotation matrix A, Equation (A1)
ε	oblateness parameter, $3\mu J_2 R_e^2/2$
θ	true anomaly
κ	drag parameter, $CA/(2m)$
μ	Earth's gravitational parameter, $3.9860 \times 10^{14} m^3/s^2$
ν	angle, $L - L_0$
ρ	air density
τ	angle, $\theta - M$
ω	argument of perigee
Δ	difference operator, $\Delta a = a_p - a$ for an arbitrary quantity a
Ω	longitude of ascending node

Additional less important symbols are defined throughout the text. Subscripts o, p refer to initial conditions and quantities belonging to the probe respectively while the station's parameters carry no subscript. The superscript $\cdot$ designates the derivative with respect to time.

1. Introduction

Subsatellites are natural candicates for future Space Lab experiments allowing the simultaneous monitoring of the physical environment in a large spatial region around the Shuttle. A detailed study on the scientific objectives and technical feasibility of an AMPS (Atmosphere, Magnetosphere, and Plasmas in Space) subsatellite payload has been carried out by ESA (Duchoissois and Dale, 1975).

The orbital characteristics of subsatellite trajectories relative to a moving reference station (e.g. Space Lab) in orbit have been studied since about 1960. By expansion of the gravitational potential in the neighborhood of the station Clohessy and Wiltshire (1960) derived a set of linear differential equations describing the relative motion in an approximate manner for small separation distance. Notwithstanding the many important improvements which have been proposed afterwards (see literature review, Van der Ha, 1980), an essential drawback of this approach is the nonuniform validity of the approximate solution as the separation distance increases.

On the other hand, a uniformly valid description of the relative motion can be obtained if the two satellites are considered to be moving in two independent orbits around their common center of attraction. The relative trajectory of one satellite with respect to the other may then be obtained by somehow subtracting the two individual orbits. This approach, however, may lead to an often unacceptable loss of precision due to the numerical subtraction of almost equal quantities: the difference of two numbers each having n significant digits with the first m of these being identical

will have not more than $n-m$ significant digits. For obtaining a full-precision description of the relative motion one should formulate the problem in terms of difference quantities throughout. The essence of this methodology dates back to Encke's method of special perturbations (see Nacozy and Szebehely, 1976). Lancaster (1970) was probably the first to employ this approach in relative motion studies. Considering unperturbed co-planar elliptic orbits Van der Ha (1980) presented an exact analytical solution expressed in terms of relative elements which themselves can be determined directly from the launching conditions. Also it was indicated how arbitrary perturbations acting on both satellites could be incorporated by allowing the station's orbital parameters as well as the relative elements to be slowly varying.

In the present paper a general exact theory for the three-dimensional perturbed relative motion is presented. In addition to the six orbital elements describing the perturbed motion of the station six relative elements are introduced which represent the instantaneous differences between the orbital parameters of the probe as compared to those of the station. Transformations between the relative state of the subsatellite, i.e. the relative position and velocity components taken in the local reference frame moving along with the station, and the relative elements are determined. This allows on one hand the calculation of the relative elements from the launching or initial conditions and on the other hand the determination of the physical state in terms of relative position and velocity from the instantaneous relative elements.

The evolution of the relative motion under arbitrary perturbing forces is found by integrating the twelve differential equations for the variation of the station's orbital elements and the relative elements. These equations contain six force components, i.e. the three local components of the perturbing force acting on the station and the three relative components representing the instantaneous differences between the respective local perturbing force components acting on the probe and those exerted on the station. In this manner also the subtraction of almost equal perturbing forces is circumvented. The Gauss formulation of perturbation equations (i.e. the perturbing forces enter through their local components rather than in terms of a disturbing function) is chosen in order to allow the inclusion of non-conservative and time-dependent perturbations. Although the canonical formulation can be adapted to include arbitrary perturbing forces by introducing so-called canonical forces (Stiefel and Scheifele, 1971, Ch. 8), it is expected that the advantage of the compactness of the canonical equations must be paid for by elaborate transformations from the actual physical perturbations to canonical forces. A formulation in terms of local force components and a non-conventional set of elements resulting in relatively compact equations is adopted here.

The general theory for the perturbed relative motion is illustrated by investigating the effects of atmospheric drag (assuming a simple exponential density model) and Earth's oblateness. The relative range and the range-rate of the probe with respect to the station can readily be expressed in terms of the relative state parameters. The resulting relative motion trajectories have been summarized in plots showing the

projected planar motion as well as in terms of range vs range-rate phase plots for a number of cases. In the absence of perturbations exact analytical representations can be obtained for the relative elements. This solution contains an infinite series representation for the true anomaly minus the mean anomaly and has essentially the same appearance as the one for the planar case derived before (Van der Ha, 1980).

2. Transformations Between Various State Representations

Three different state representations will be employed for describing various aspects of the motions of station and probe. In the *inertial* formulation the states of the two satellites are referred to the inertial X_1, X_2, X_3 reference frame with origin at the center of the Earth. In order to prevent the loss of precision inherent in the subtraction of two almost equal numerical quantities the convention of representing the state of the probe by difference-variables relative to the station's state is adopted. Thus, the complete state of the two satellites is described by the twelve-dimensional vector:

$$(\mathbf{r}, \mathbf{v}\,; \Delta\mathbf{r}, \Delta\mathbf{v}). \tag{1}$$

If one would need the state of the probe itself in the calculations it can be obtained in explicit form using the representation given in (1) by a simple addition of the components of the state vector:

$$(\mathbf{r}_p, \mathbf{v}_p) = (\mathbf{r} + \Delta\mathbf{r}, \mathbf{v} + \Delta\mathbf{v}). \tag{2}$$

The second formulation which is particularly useful in subsatellite studies provides a description of the *relative* motion of the probe within a local reference frame moving along with the station. Thereto the local x, y, z frame (Figure 1) with the x-axis along the station's instantaneous local vertical, the y-axis along its local horizontal and the z-axis normal to its orbital plane is introduced. It must be emphasized that at all times the station's $\mathbf{r}$ and $\mathbf{v}$ vectors will lie within the local x, y plane, i.e. the osculating plane. The probe's relative state in this frame is described by the six-dimensional vector $(\mathbf{x}, \dot{\mathbf{x}}) = (x, y, z, \dot{x}, \dot{y}, \dot{z})$, denoting the relative position and velocity vectors of the probe in the station's local reference frame. The complete state of both station and probe can thus also be represented by the twelve-vector:

$$(\mathbf{r}, \mathbf{v}; \mathbf{x}, \dot{\mathbf{x}}), \tag{3}$$

where its hybrid character should be kept in mind: the former six components are referred to the inertial frame whereas the latter six are taken in the local frame.

The third formulation to be employed here makes use of orbital elements and is particularly suited for describing the perturbed motions of station and probe. The state of the station can directly be represented by a set of six orbital elements. In order to avoid the subtraction of almost equal quantities *relative elements* are introduced to describe the state of the probe relative to that of the station. The six relative elements represent the instantaneous differences between the orbital elements of probe and

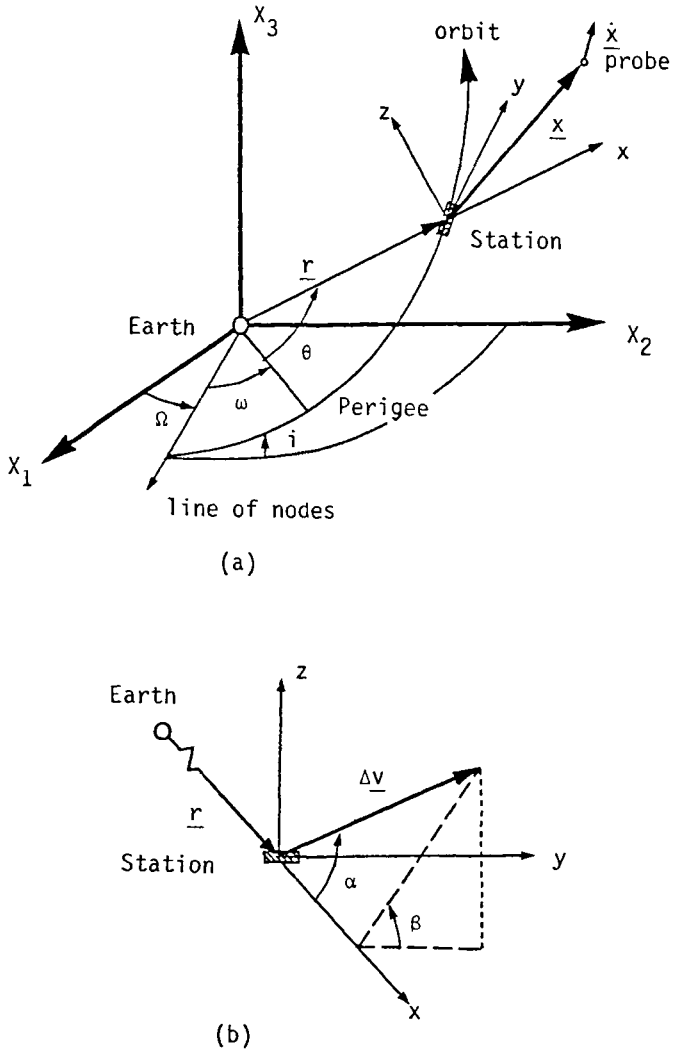

Fig. 1. (a) Station's orbital geometry and relative state vectors of probe. (b) Visualisation of Δv with cone and clock angles α, β.

station. Thus, the twelve-vector:

$$(\mathbf{a}, \Delta\mathbf{a}), \tag{4}$$

where **a** denotes a suitable collection of six orbital elements, is fully equivalent to the two previous formulations in describing the complete state of the two satellites.

Subsequently, the transformations between the three state representations will be discussed. The inertial formulation plays a central role since the transformations between the relative state and the elements employ it as a stepping stone.

2.1. Connection between inertial and relative formulations

The transformations between the inertial state vector $(\Delta\mathbf{r}, \Delta\mathbf{v})$ and the relative state $(\mathbf{x}, \dot{\mathbf{x}})$ are described by the kinematical relationships:

$$\Delta\mathbf{r} = \mathbf{x}, \quad \Delta\mathbf{v} = \dot{\mathbf{x}} + \mathbf{w} \times \mathbf{x}, \tag{5}$$

where $\mathbf{w}$ represents the instantaneous rotation vector of the local frame with respect to inertial space. Writing $\mathbf{V} = \mathbf{w} \times \mathbf{x}$ and expanding the vectors of Equations (5) in their respective components leads to the identities:

$$\begin{aligned} x_j &= \alpha_{jk}\Delta r_k, \quad \dot{x}_j = \alpha_{jk}\Delta v_k - V_j, \quad j = 1, 2, 3. \\ \Delta r_j &= \alpha_{kj}x_k, \quad \Delta v_j = \alpha_{kj}(\dot{x}_k + V_k), \quad j = 1, 2, 3. \end{aligned} \tag{6}$$

Here, it should be understood that automatic summation over identical subscripts takes place. In order to distinguish components referred to the local axes from those with respect to inertial axes the subscripts 1, 2, 3 should be read as x, y, z in the former case. The components of the rotation matrix $A = [\alpha_{jk}]$ and its transpose $A^T = [\alpha_{kj}]$, $j, k = 1, 2, 3$, depend on the instantaneous state of the station and are given in Appendix I.

Next, the local components of the vector $\mathbf{V} = \mathbf{w} \times \mathbf{x}$ are determined for arbitrary perturbed motion. Thereto the instantaneous velocity and angular momentum (per unit mass) vectors are considered. Recognizing that at each instant both the velocity and the position vector of the station are lying in the local x, y plane because that is how it was chosen, one obtains the following expressions for the velocity and angular momentum vectors:

$$\begin{aligned} \mathbf{v} &= \dot{\mathbf{r}} = \dot{r}\mathbf{u}_x + \mathbf{w} \times \mathbf{r} = \dot{r}\mathbf{u}_x + rw_z\mathbf{u}_y, \\ \mathbf{h} &= \mathbf{r} \times \mathbf{v} = r^2 w_z \mathbf{u}_z. \end{aligned} \tag{7}$$

In order that the z component of $\mathbf{v}$ vanishes $w_y = 0$ had to be imposed. From the second result it is seen that $w_z = h/r^2$. The remaining component w_x can be determined by studying the rate of change of $\mathbf{h}$ in the local frame:

$$\dot{\mathbf{h}} = \dot{h}\mathbf{u}_z + \mathbf{w} \times \mathbf{h} = \dot{h}\mathbf{u}_z - hw_x\mathbf{u}_y, \tag{8}$$

while on the other hand one finds from Newton's second law for perturbed motion, i.e. $\dot{\mathbf{v}} = -\mu\mathbf{r}/r^3 + \mathbf{F}$, that:

$$\dot{\mathbf{h}} = \mathrm{d}(\mathbf{r} \times \mathbf{v})/\mathrm{d}t = \mathbf{r} \times \dot{\mathbf{v}} = r(F_y\mathbf{u}_z - F_z\mathbf{u}_y). \tag{9}$$

Comparison of the expressions in Equations (8) and (9) produces in addition to $\dot{h} = rF_y$ the x component of $\mathbf{w}$: $w_x = rF_z/h$. The local components of the vector $\mathbf{V} = \mathbf{w} \times \mathbf{x}$ appearing in Equations (6) follow now immediately:

$$V_x = -yh/r^2; \quad V_y = xh/r^2 - zrF_z/h; \quad V_z = yrF_z/h. \tag{10}$$

These results show that in perturbed motion the transformations between the inertial and relative representations for the probe's relative velocity in Equations (6) depend explicitly on the instantaneous normal component of the perturbing force. Also it may be noted that the quantities r and h appearing in Equations (10) are osculating, i.e. the effects of the perturbing forces must be taken into account for determining the evolution of their instantaneous values.

2.2. Transformation between inertial and element formulation

The transformation from the inertial state vector $(\mathbf{r}, \mathbf{v}; \Delta\mathbf{r}, \Delta\mathbf{v})$ to the element representation $(\mathbf{a}; \Delta\mathbf{a})$ is studied now. Since the classical element formulation has singularities for near-zero eccentricity and/or inclination in the equations for $\dot{\omega}$ and $\dot{\Omega}$ (Fitzpatrick, 1970, Ch. 7), a non-conventional set of elements which avoids these difficulties is introduced:

$$\mathbf{a} = (h, f, g, j, k, L). \tag{11}$$

In terms of the classical orbital elements, i.e. $\mathbf{c} = (l, e, \omega, i, \Omega, \theta)$ with θ being the true anomaly, the elements in Equation (11) are defined as follows:

$$h = \sqrt{\mu l}; \quad f = e\cos\theta; \quad g = e\sin\theta;$$
$$j = \tan(i/2)\cos\Omega; \quad k = \tan(i/2)\sin\Omega; \quad L = \theta + \omega + \Omega. \tag{12}$$

It should be emphasized that f, g, as well as the true longitude L, are in general fast variables, i.e. their rate of change does not vanish in the absence of perturbations. This would imply that a smaller stepsize would be required in numerical integration as compared to the case where all elements are slowly-varying. In an important special case, namely when the eccentricity remains of the same order of smallness as the perturbing forces throughout the interval of interest, one may safely treat the elements f and g as if they were slow elements. Furthermore, the true longitude L may be separated into two parts, $L(t) = L_u(t) + \lambda(t)$, where $L_u(t)$ represents the true longitude of the corresponding unperturbed orbit emanating from the same initial conditions as the actual perturbed orbit. The slowly-varying deviation of $L(t)$ from $L_u(t)$ is then described by $\lambda(t)$ which vanishes identically in the absence of perturbations. It should be noted that for general eccentric orbits also the elements f and g can be treated in a similar manner so that for numerical purposes the set of elements defined in Equations (12) can readily be turned into a slowly-varying set for arbitrary eccentricity. The inverse relations of Equations (12) expressing the classical elements in terms of the non-conventional set become simply:

$$l = h^2/\mu; \quad e = \sqrt{f^2 + g^2}; \quad \theta = \arctan(g/f);$$
$$i = 2\arctan(\sqrt{j^2 + k^2}); \quad \Omega = \arctan(k/j); \quad \omega = L - \theta - \Omega. \tag{13}$$

In addition to the six station elements in Equation (11) a set of six *relative elements* representing the instantaneous differences between probe's and station's orbital parameters is introduced for obtaining a complete description of the motion of the two statellites:

$$\Delta\mathbf{a} = (\Delta h, \Delta f, \Delta g, \Delta j, \Delta k, \Delta L). \tag{14}$$

The relations expressing the twelve elements $(\mathbf{a}, \Delta\mathbf{a})$ in terms of the twelve inertial vector components $(\mathbf{r}, \mathbf{v}; \Delta\mathbf{r}, \Delta\mathbf{v})$ and the converse expressions are fairly lengthy and are summarized in Appendix II.

Finally, it is mentioned that the transformations from the relative formulation to the element representation (as well as the converse) can now be constructed in two steps: first, one transforms from the relative to the inertial formulation and subsequently to elements.

3. Variation of Elements and Relative Elements

In the present section differential equations will be formulated which describe the rate of change of the station's elements as well as that of the relative elements under arbitrary perturbing forces acting on both station and probe. The formulation adopted here uses the Gauss form of perturbation equations so that no restrictions are imposed on the nature of the perturbing forces as they enter the equations through their instantaneous components projected upon the local axes. It is clear that the six perturbation equations for the station's motion will contain the three local components (F_x, F_y, F_z) of the perturbing force acting on the station. Similarly, the probe's motion is affected by perturbing forces with resulting components (F_{px}, F_{py}, F_{pz}) along its local axes. In order to avoid the subtraction of almost equal quantities one should not use $\mathbf{F}_p$ itself but the instantaneous difference force components $(\Delta F_x, \Delta F_y, \Delta F_z)$. It must be emphasized that ΔF_x should not be interpreted as the component of $\mathbf{F}_p - \mathbf{F}$ along the station's local vertical, but as the difference between the probe's perturbing force component along its local vertical (x_p-axis), F_{px}, and the station's perturbing force projected on the station's local vertical (x-axis), F_x.

The six perturbation equations for the station in terms of the set of elements given in Equation (11) can be derived from the classical Lagrange Planetary equations (Fitzpatrick, 1970, Ch. 7) or also directly from Newton's second law:

$$\begin{aligned}
\dot{h} &= rF_y, \\
\dot{f} &= -hg/r^2 + 2hF_y/\mu, \\
\dot{g} &= hf/r^2 + hF_x/\mu + grF_y/h, \\
(\dot{j}) &= rF_z \cos L(1 + j^2 + k^2)/(2h), \\
\dot{k} &= rF_z \sin L(1 + j^2 + k^2)/(2h), \\
\dot{L} &= h/r^2 + rF_z(j \sin L - k \cos L)/h,
\end{aligned}$$

with

$$r = h^2/[\mu(1+f)]. \tag{15}$$

The compactness of this set of equations in comparison with the classical perturbation equations is evident. The variation of the probe's elements would be described by a similar set of equations with all quantities related to the probe since its motion can be considered to be independent from that of the station. The acceleration components F_{px}, F_{py}, and F_{pz} would be expanded along the probe's local axes. Introducing the instantaneous acceleration component differences

$$\Delta F_x = F_{px} - F_x \quad \text{(cyclic for } x, y, z), \tag{16}$$

one can formulate the equations for the variation of the relative elements by subtracting the corresponding equations for the probe and station. Care should be taken, however, that the subtraction of almost equal quantities is avoided. Therefore, the following full-precision difference-procedures are introduced for handling the subtraction of almost equal products and quotients:

$$\begin{aligned}
&\Delta(x^2) = (2x + \Delta x)\Delta x,\\
&\Delta(xy) = (y + \Delta y)\Delta x + x\Delta y,\\
&\Delta(xyz) = (z + \Delta z)\Delta(xy) + xy\Delta z,\\
&\Delta(x/y) = [\Delta x - (x/y)\Delta y]/(y + \Delta y),
\end{aligned} \tag{17}$$

where x, y, and z denote arbitrary quantities. After repeated application of the rules in Equation (17) one obtains the equations for variation of the relative elements:

$$\begin{aligned}
(\Delta h)^{\cdot} &= \Delta(rF_y),\\
(\Delta f)^{\cdot} &= -\left[(g + \Delta g)\Delta(h/r^2) + h\Delta g/r^2\right] + 2\Delta(hF_y)/\mu,\\
(\Delta g)^{\cdot} &= \left[(f + \Delta f)\Delta(h/r^2) + h\Delta f/r^2\right] + \Delta(hF_x)/\mu +\\
&\quad + \left[(g + \Delta g)\Delta G_y + G_y\Delta g\right],\\
(\Delta j)^{\cdot} &= \tfrac{1}{2}\left[(1 + J + \Delta J)\Delta G_z + G_z\Delta J\right]\cos(L + \Delta L) + \tfrac{1}{2}G_z(1 + J)\Delta(\cos L),\\
(\Delta k)^{\cdot} &= \tfrac{1}{2}\left[(1 + J + \Delta J)\Delta G_z + G_z\Delta J\right]\sin(L + \Delta L) + \tfrac{1}{2}G_z(1 + J)\Delta(\sin L),\\
(\Delta L)^{\cdot} &= \Delta(h/r^2) + (j\sin L - k\cos L)\Delta G_z +\\
&\quad + (G_z + \Delta G_z)\left[\Delta j\sin(L + \Delta L) - \Delta k\cos(L + \Delta L) + j\Delta(\sin L) -\right.\\
&\quad \left. - k\Delta(\cos L)\right],
\end{aligned}$$

with

$$\begin{aligned}
&J = j^2 + k^2; \quad G_j = rF_j/h, \quad j = y, z;\\
&\Delta J = \Delta(j^2) + \Delta(k^2);
\end{aligned}$$

$$\Delta G_j = [\Delta(rF_j) - G_j \Delta h]/(h + \Delta h), \quad j = y, z;$$

$$\Delta r = [\Delta(h^2) - h^2 \Delta f/(1+f)]/[\mu(1 + f + \Delta f)];$$

$$\Delta(h/r^2) = [\Delta h - h\Delta(r^2)/r^2]/(r + \Delta r)^2, \tag{18}$$

while $\Delta(\cos L)$ and $\Delta(\sin L)$ are given in Appendix I, Equations (A5). The set of twelve first-order differential equations in (15) and (18) describe in an exact manner and with full precision the motion of the station as well as the motion of the probe relative to the station under arbitrary perturbing forces acting on both bodies. If one wants to evaluate the effect of a particular perturbing force on the motion of the two satellites one needs to calculate the six perturbation components $(F_x, F_y, F_z, \Delta F_x, \Delta F_y, \Delta F_z)$ with the use of the rules specified in Equations (17) and substitute these expressions in the system of Equation (15) and (18). In later sections this procedure will be illustrated by means of a few realistic perturbing forces: Earth's oblateness and air drag.

4. Unperturbed Relative Motion

If the perturbing forces are assumed to be absent one can determine exact representations for the relative motion without loss of precision. The slow orbital elements h, j, k as well as the corresponding relative elements $\Delta h, \Delta j, \Delta k$ will remain constant in this case and can be determined from the initial conditions $(\mathbf{r}_0, \mathbf{v}_0; \Delta\mathbf{r}_0, \Delta\mathbf{v}_0)$ by means of Equations (A6) in Appendix II. Also the initial values of the non-constant orbital parameters are obtained from Equations (A6): $f_0, g_0, L_0; \Delta f_0, \Delta g_0, \Delta L_0$. The objective is now to determine the evolution of these six elements as a function of time. Thereto these elements are written in terms of $v = L - L_0 = \theta - \theta_0$:

$$f = f_0 \cos v - g_0 \sin v, \quad g = f_0 \sin v + g_0 \cos v,$$

$$\Delta f = \Delta f_0 \cos(v + \Delta v) - \Delta g_0 \sin(v + \Delta v) - 2f \sin^2(\Delta v/2) - g \sin(\Delta v),$$

$$\Delta g = \Delta f_0 \sin(v + \Delta v) + \Delta g_0 \cos(v + \Delta v) - 2g \sin^2(\Delta v/2) + f \sin(\Delta v), \tag{19}$$

with $\Delta v = \Delta L - \Delta L_0$. It is seen that only L and ΔL still need to be determined. The station's true longitude can be written as

$$L = \theta + L_0 - \theta_0, \quad \theta_0 = \arctan(g_0/f_0), \tag{20}$$

while the station's true anomaly as a function of time follows from Kepler's equation.

The derivation of ΔL with full precision for elliptic orbits is a little lengthy but straight-forward. Use will be made of the variable τ representing the instantaneous difference between the station's true and mean anomaly:

$$\tau = \theta - M = \sum_{j=1}^{\infty} C_j \sin(jM), \tag{21}$$

where the coefficients C_j can be expressed in terms of Bessel functions containing

multiples of the eccentricity as arguments, Brouwer and Clemence (1961), Ch. 2, Equation (74). For practical applications when the eccentricities are less than say 0.5 the series expansion

$$C_j = \sum_{m=0}^{\infty} c_{jm}(e/2)^{2m+j}, \quad j = 1, 2, \ldots, \tag{22}$$

is more convenient. The coefficients c_{jm} have been evaluated for $j = 1, 2, \ldots, 16$ and $m = 1, 2, \ldots, 8 - [j/2]$ by means of a formula manipulating computing language (SYMBAL), Van der Ha (1980). The relative element ΔL can now be written as

$$\Delta L = \Delta\tau + \Delta M + \Delta L_0 - \Delta\theta_0, \tag{23}$$

where all terms can be expressed in known quantities:

$$\Delta\theta_0 = \arctan\{(f_0\Delta g_0 - g_0\Delta f_0)/(f_0^2 + g_0^2 + f_0\Delta f_0 + g_0\Delta g_0)\},$$

$$\Delta M = \Delta M_0 + t\Delta n,$$

$$\Delta M_0 = \Delta E_0 - \Delta e \sin(E_0 + \Delta E_0) - 2e \sin(\Delta E_0/2)\cos(E_0 + \Delta E_0/2),$$

$$E_0 = 2 \arctan[S \tan\theta_0/2)], \quad S = \sqrt{(1-e)/(1+e)}, \quad e = \sqrt{f_0^2 + g_0^2},$$

$$\Delta E_0 = \{\Delta S \sin[(\theta_0 + \Delta\theta_0)/2]\cos(\theta_0/2) + S\sin(\Delta\theta_0/2)\}/$$
$$\{\cos[(\theta_0 + \Delta\theta_0)/2]\cos(\theta_0/2) + S(S + \Delta S)\sin[(\theta_0 + \Delta\theta_0)/2]\times$$
$$\times \sin(\theta_0/2)\},$$

$$\Delta S = -2\Delta e/[(1+e)\sqrt{1-(e+\Delta e)^2} + (1 + e + \Delta e)\sqrt{1-e^2}],$$

$$\Delta e = [\Delta(f_0^2) + \Delta(g_0^2)]/[e + \sqrt{(f_0 + \Delta f_0)^2 + (g_0 + \Delta g_0)^2}],$$

$$\Delta n = -A\sqrt{\mu/a^3}[A^2 + 3(1-A)]/[1 + (1-A)^{3/2}],$$

$$A = \Delta a/(a + \Delta a), \quad a = h^2/[\mu(1-e^2)],$$

$$\Delta a = \{\Delta(h^2) + h^2\Delta(e^2)/(1-e^2)\}/\{\mu[1-(e+\Delta e)^2]\},$$

$$\Delta\tau = \sum_{j=1}^{\infty} \{2C_j \sin[j\Delta M/2]\cos[j(M + \Delta M/2)] + \Delta C_j \sin[j(M + \Delta M)]\},$$

$$\Delta C_j = \Delta e \sum_{m=0}^{\infty} \{c_{jm} 2^{-2m-j} \sum_{k=1}^{2m+j} [(e + \Delta e)^{k-1} e^{2m+j-k}]\}, \quad j = 1, 2, \ldots \tag{24}$$

The validity of this solution is restricted only by the domain of convergence of the series expansion of Equations (22) and 24): $e < 0.6627434$. A discussion of the accuracy of the results as a function of the eccentricity is given by Van der Ha (1980) where the co-planar case was studied. Naturally, those accuracies remain valid also for the present solution.

It may be useful to briefly summarize how to employ the results in an actual application:

(i) The station's initial state is given in terms of either its orbital elements or its $\mathbf{r}_0, \mathbf{v}_0$ vectors in inertial space. Also the initial position and velocity difference vectors $\Delta\mathbf{r}_0$ and $\Delta\mathbf{v}_0$ of the probe with respect to the station are provided. (If the relative position and velocity vectors $\mathbf{x}_0$ and $\dot{\mathbf{x}}_0$ were given, the latter transformation of Equations (6) would produce $\Delta\mathbf{r}_0$ and $\Delta\mathbf{v}_0$).

(ii) The initial twelve orbital elements can be calculated by means of Equations (A6).

(iii) While six of these elements remain constant throughout, the remaining elements can be determined at an arbitrary time t from Equations (24).

(iv) Since the instantaneous elements are known at time t one can obtain the corresponding state vector $(\mathbf{r}, \mathbf{v}; \Delta\mathbf{r}, \Delta\mathbf{v})$ using Equations (A8) and (A10),

(iv) If the relative state $(\mathbf{x}, \dot{\mathbf{x}})$ is needed at time t the former transformation in Equations (6) should be applied next.

5. Perturbed Relative Motion

The exact theory for perturbed relative motion based on the variation of the relative elements will be applied to the most relevant perturbing forces for near-Earth satellite orbits, namely air drag and Earth's oblateness. The objective is to obtain expressions for the components F_j and $\Delta F_j, j = x, y, z$ appearing in Equations (15) and (18) in terms of the instantaneous elements $(\mathbf{a}, \Delta\mathbf{a})$.

5.1. Air drag perturbations

Although the formulation itself does not impose any restriction on the nature or complexity of the particular air density model, the algebra in calculating the difference force components becomes extremely cumbersome for realistic air density models accounting for the influences of the diurnal bulge, solar and geomagnetic activity. For the purpose of illustration a simple stationary exponential density model is adopted here:

$$\rho = \rho(r) = \bar{\rho}\exp\left[-(r - \bar{r})/H\right], \tag{25}$$

where $\bar{\rho} = \rho(\bar{r})$ is the given constant density at some suitable reference altitude and H designates the presumably constant density scale height. Its value may be chosen differently for different reference altitudes $\bar{r}$ in order to account for its tendency to increase at higher altitude. The perturbing acceleration of the station induced by air drag is written as:

$$\mathbf{F} = -\rho C(A/m)v\mathbf{v}/2, \tag{26}$$

where C stands for the drag coefficient ($C = 2.2$ for a spherical satellite in free-molecule

flow) and A/m is the area/mass ratio of the station. It may be mentioned that in expression (26) the speed of the ambient air due to the Earth's rotation is neglected in comparison to the satellite's velocity. Also the effect of the Earth's oblateness on the shape of equidensity surfaces in the atmosphere is ignored. Writing $\mathbf{v} = \dot{r}\mathbf{u}_x + (h/r)\mathbf{u}_y$, Equations (8), one obtains the following local components of $\mathbf{F}$:

$$F_x = -\rho\kappa v\dot{r}, \quad F_y = -\rho\kappa v h/r, \quad F_z = 0, \tag{27}$$

with drag parameter $\kappa = CA/(2m)$ and $v = [\dot{r}^2 + (h/r)^2]^{1/2}$.

The instantaneous differences in the local force components of the probe compared to those of the station can be calculated with full precision from Equations (27) using the rules formulated in Equations (17):

$$\begin{aligned} \Delta F_x &= -[\dot{r} + \Delta(\dot{r})]\Delta(\rho\kappa v) - \rho\kappa v\Delta(\dot{r}), \\ \Delta F_y &= -[h/r + \Delta(h/r)]\Delta(\rho\kappa v) - \rho\kappa v\Delta(h/r), \end{aligned} \tag{28}$$

where the explicit expressions of r, $\dot{r}$ and $\Delta(\dot{r})$ in terms of elements are given in Equations (A7), while $\Delta(h/r)$ and $\Delta(\rho\kappa v)$ can be broken up as shown in Equations (17) in terms of Δh, Δr and $\Delta\rho$, $\Delta\kappa$ and Δv, respectively. The difference in orbital radius can then be expressed in elements and relative elements as in Equations (18). The density at r_p, i.e. the probe's position, can be obtained from Equation (25) when replacing r by r_p and taking the same reference density $\bar{\rho}$ and scale height H as for the station. If there exists a large discrepancy between the perigee heights of station and probe intermediate reference values for $\bar{\rho}$ and H should be chosen. The following exact representation for the density difference can be calculated from Equation (25):

$$\Delta\rho = -2\rho \exp[-\Delta r/(2H)] \sinh[\Delta r/(2H)]. \tag{29}$$

The expressions for Δv and $\Delta\kappa$ are given by:

$$\begin{aligned} \Delta v &= \{[2\dot{r} + \Delta(\dot{r})]\Delta(\dot{r}) + [2h/r + \Delta(h/r)]\Delta(h/r)\}/(v + v_p), \\ v_p &= \{[\dot{r} + \Delta(\dot{r})]^2 + [h/r + \Delta(h/r)]^2\}^{1/2}, \\ \Delta\kappa &= [C + \Delta C)\Delta(A/m) + (A/m)\Delta C]/2, \end{aligned} \tag{30}$$

which can further be reduced in terms of ΔA and Δm. It may be noted that for large differences in A/m of probe and station $\Delta\kappa$ can be calculated by direct subtraction since there is no danger of loss of precision in that case.

5.2. Earth's oblateness perturbations

Taking the inertial X_3 axis normal to the equatorial plane the disturbing potential (per unit mass) due to the Earth's oblateness is given by:

$$V = -\varepsilon[1/3 - (X_3/r)^2]/r^3, \tag{31}$$

where $\varepsilon = 3\mu J_2 R_e^2/2$. The perturbing acceleration becomes thus:

$$\mathbf{F} = -\bar{v}V = -\varepsilon[1 - 5(X_3/r)^2]\mathbf{r}/r^5 - 2\varepsilon X_3 \mathbf{U}_3/r^5. \tag{32}$$

The local components of this expression are

$$F_x = -\varepsilon(1 - 3\alpha_{13}^2)/r^4, \quad F_y = -2\varepsilon\alpha_{13}\alpha_{23}/r^4, \quad F_z = -2\varepsilon\alpha_{13}\alpha_{33}/r^4, \tag{33}$$

where $\alpha_{j3} = (\mathbf{u}_j, \mathbf{U}_3), j = x, y, z$, can be expressed in the instantaneous elements, Appendix I. The three difference components can be calculated again using the rules of Equations (17). One finds:

$$\begin{aligned}
\Delta F_x &= \varepsilon[3\Delta(\alpha_{13})^2 + (1 - 3\alpha_{13}^2)\Delta(r^4)/r^4]/(r + \Delta r)^4, \\
\Delta F_y &= 2\varepsilon[\alpha_{13}\alpha_{23}\Delta(r^4)/r^4 - \Delta(\alpha_{13}\alpha_{23})]/(r + \Delta r)^4, \\
\Delta F_z &= 2\varepsilon[\alpha_{13}\alpha_{33}\Delta(r^4)/r^4 - \Delta(\alpha_{13}\alpha_{33})]/(r + \Delta r)^4,
\end{aligned} \tag{34}$$

where $\Delta(\alpha_{13}\alpha_{j3}), j = 1, 2, 3$, can be expressed in the elements and relative elements by means of Equations (17) and Equations (A5), whereas

$$\Delta(r^4)/r^4 = \sigma(4 + 6\sigma + 4\sigma^2 + \sigma^3); \quad \sigma = \Delta r/r. \tag{35}$$

Higher zonal harmonics and also tesseral harmonics could be included in a similar manner. Their effects on the relative motion will be negligible in general.

6. Discussion of Results

The theory presented above has been programmed and the resulting relative motion patterns have been established for a variety of test cases. The validity of the results for the unperturbed case as well as of those under air drag and oblateness perturbations was confirmed through comparisons with the motion of the two individual satellites derived from a different independent orbit generator. Since it was observed that the relative motion is hardly affected by the parameters of the station's orbit as long as its eccentricity is small (< 0.01) a typical station orbit with orbital elements $a = 6778$ km, $i = 30°$ and $e = \Omega = 0$, will be taken in the following.

The influence of the Earth's oblateness on the relative motion is illustrated in Figure 2 for a subsatellite launched with $\Delta v = 10$ ms^{-1} under cone and clock angles $\alpha = 30°$ and $\beta = 60°$. These angles can be visualized with the aid of Figure 1b and lead immediately to the initial relative state:

$$\mathbf{x}_0 = 0; \quad \dot{\mathbf{x}}_0 = \Delta v(\cos\alpha\,\mathbf{u}_x + \sin\alpha\cos\beta\,\mathbf{u}_y + \sin\alpha\sin\beta\,\mathbf{u}_z), \tag{36}$$

since $\dot{\mathbf{x}}$ equals $\Delta\mathbf{v}$ when $\mathbf{x} = \mathbf{0}$, Equations (5). Figure 2a shows the projected (in the station's instantaneous orbital plane) relative motion pattern of the probe as seen from the station. It should be recognized that the x, y reference plane is not inertially fixed under oblateness perturbations: the F_z force component, Equations (33), produces a slow rotation of the x, y plane about the station's instantaneous local vertical i.e. the x-axis. The same case as in Figure 2a is shown in Figure 2b in a different way:

here the range and range-rate evolution are plotted against one another in a phase-plane manner. The variables R and $\dot{R}$ are the most natural ones for describing three-dimensional subsatellite trajectories since they represent directly measurable quantities. Their values in Figure 2b are derived from the following simple expressions in terms of the relative state vectors $\mathbf{x}$ and $\dot{\mathbf{x}}$:

$$R = |\mathbf{x}|; \quad \dot{R} = (\mathbf{x}, \dot{\mathbf{x}})/R. \tag{37}$$

It is seen from Figure 2 that the J_2-perturbed and the unperturbed relative trajectories practically coincide over the first ten revolutions. This close agreement (at least two common digits in the range distance) was also observed in other test cases and is due to the fact that the difference in the J_2 induced perturbing forces acting on probe and station is an order of magnitude smaller than the individual J_2 perturbations exerted on each body. This may be seen from Equations (34) where $\Delta \mathbf{F}$ is proportional to $\varepsilon \Delta r/r$ with Δr much smaller than r. Thus, the variation of the relative elements which is induced exclusively by difference quantities is much slower than that of each of the two sets of orbital elements separately.

More interesting than the oblateness effects are the drag induced perturbations of the relative motion trajectories. Nowadays, it is common practice to derive air densities from the exospheric temperature T_∞ which itself is determined from empirical relations containing, principally, solar and geomagnetic activity levels as well as the local solar time governing the diurnal heating of the atmosphere (Jacchia, 1977). Taking the station's orbital radius as reference height, i.e. $\bar{r} = 400 + R_e$ km, the values summarized in Table I for air densities and scale heights at low, middle and high values of exospheric temperature are derived from Jacchia, 1977.

TABLE I

Densities and scale heights for a few values of T_∞ at $\bar{r} = 400$ km altitude

T_∞(K)	$\bar{\rho}$(kg/m^3)	H(km)
Low : 600	2.12×10^{-13}	37.75
Middle : 1000	3.11×10^{-12}	55.92
High : 2000	2.48×10^{-11}	90.48

Figure 3 shows the relative motion under the same launching conditions as in Figure 2 but including drag perturbations for the high exospheric temperature situation. Although it is not realistic to assume a constant T_∞ over the duration of ten revolutions because of considerable local fluctuations (e.g. the diurnal effect), the results may nevertheless he representative of the actual trajectory described when the mean exospheric temperature above the orbit paths amounts to 2000 K and the fluctuations around this average value are within reasonable bounds. The values for the drag parameters of probe and station were taken identical in Figure 3. The lower value

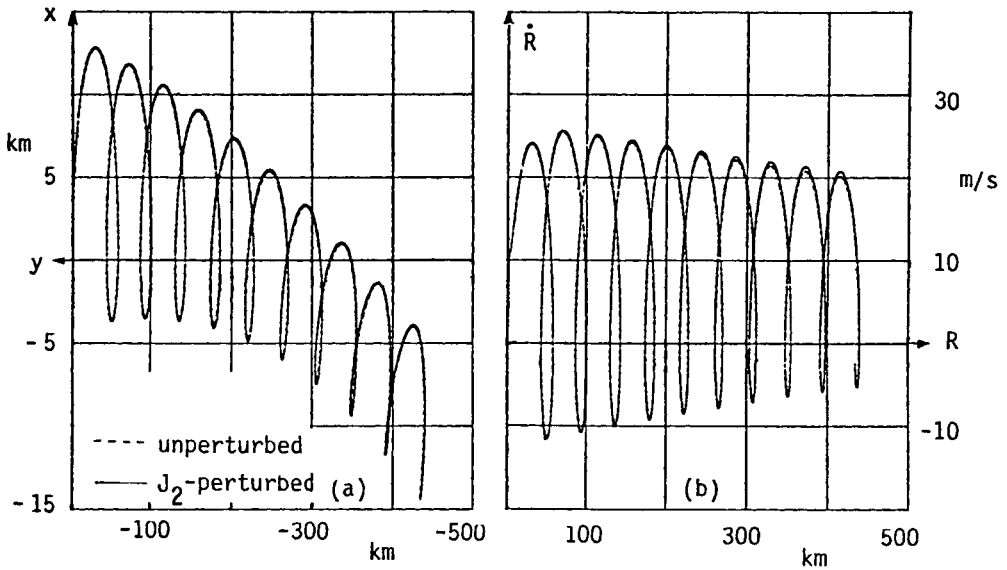

Fig. 2. Unperturbed and J_2-perturbed relative trajectory, launched with $\Delta v = 10\,\mathrm{ms}^{-1}$, $\alpha = 30°$, $\beta = 60°$. (a) projected planar motion; (b) range vs range-rate.

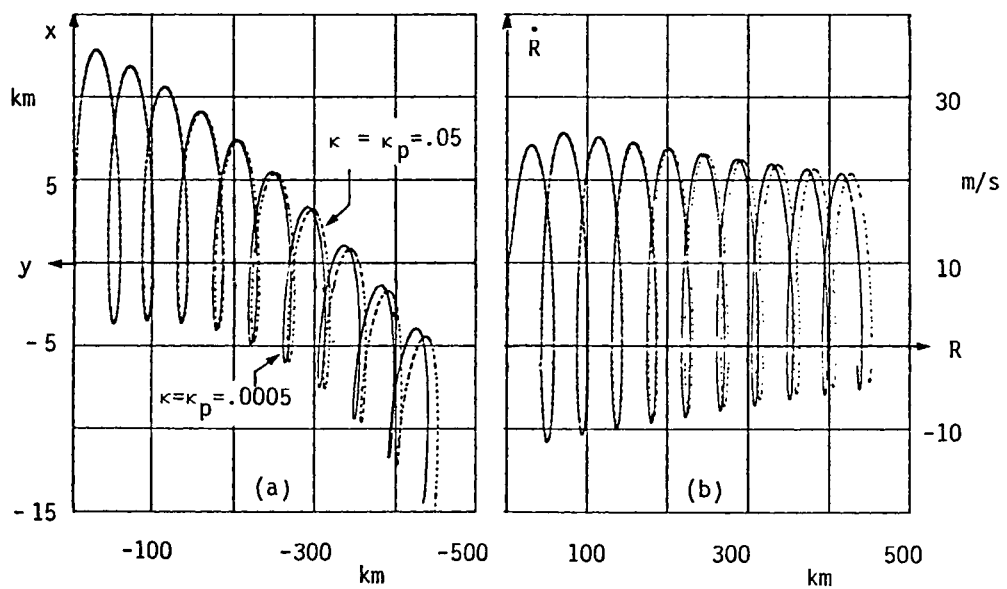

Fig. 3. Drag-perturbed relative trajectory, launched with $\Delta v = 10\,\mathrm{ms}^{-1}$, $\alpha = 30°$, $\beta = 60°$, for identical drag parameters. (a) projected planar motion; (b) range vs range-rate.

$\kappa = .0005$ would correspond to the actual value for the Space Shuttle flying in a minimum drag attitude. Whereas the solid curve essentially coincides with the unperturbed motion in Figure 2, the dotted curve representing a 100 times higher value of $\kappa = \kappa_p$ shows a noticeable deviation: since in this case the perturbing forces themselves are larger also their differences are correspondingly larger, Equation (28). If the middle or low density values of Table I were chosen a negligible deviation from the patterns of Figure 2 would be the result even if the large value $\kappa = \kappa_p = .05$ were taken. It can be understood why the dotted curve will tend to move farther away from the station than the solid line. Since the probe moves at a higher mean altitude due to the positive energy increment obtained at launch its loss of energy due to drag will be less than that of the station. This differential energy loss is naturally more significant for higher values of the drag parameter and leads to the lower mean orbital rate for the probe as displayed by the dotted curves in Figure 3.

More dramatic deviations from the unperturbed relative motion patterns are observed when the drag parameters of probe and station are different: in that case there will be a considerable difference in the respective drag forces even when the two satellites are close to one another. Taking coplanar trajectories and an intermediate air density ($T_\infty = 1000$ K), Figure 4 shows two cases where the station's drag parameter κ is 100 times as large as κ_p. Since the station's energy loss is correspondingly larger than that of the probe a continual relative decrease in the probe's mean angular rate and an accelerating drift pattern will be the result. In Figure 4a the probe is launched in the local vertical direction so that there is no essential difference in the angular rates of station and probe if their drag parameters are identical as is illustrated by the motionless elliptical pattern. In Figure 4b the probe has been launched into a higher energy orbit so that in the case of identical drag parameters a constantly drifting pattern appears, i.e. the dotted curve. If $\kappa > \kappa_p$ the energy discrepancy will grow and the drift will accelerate continually as shown by the solid curve.

In Figure 5 the reverse situation where κ_p is 100 times larger than κ is illustrated. The initially higher differential energy of the probe is quickly dissipated due to its higher sensitivity to drag. As the probe continues to lose more energy than the station, a very interesting reversal of the relative trajectory is observed when the probe's mean angular rate surpasses that of the station, Figure 5a. By increasing the initial energy difference the reversal can be postponed to any arbitrary time. Figure 5b shows a case where the probe after ten revolutions very nearly returns to the station. Due to its lower energy as compared to the station automatic rendez-vous may be hard to accomplish. Nevertheless, these trajectories could be of practical importance as they allow the later retrieval of a (possibly tethered) subsatellite by the Shuttle with relatively little manoeuvering. By choosing suitable launching conditions based on energy considerations any arbitrary time interval between launch and retrieval could be accommodated.

The effect of different exospheric temperature on the relative trajectories is shown

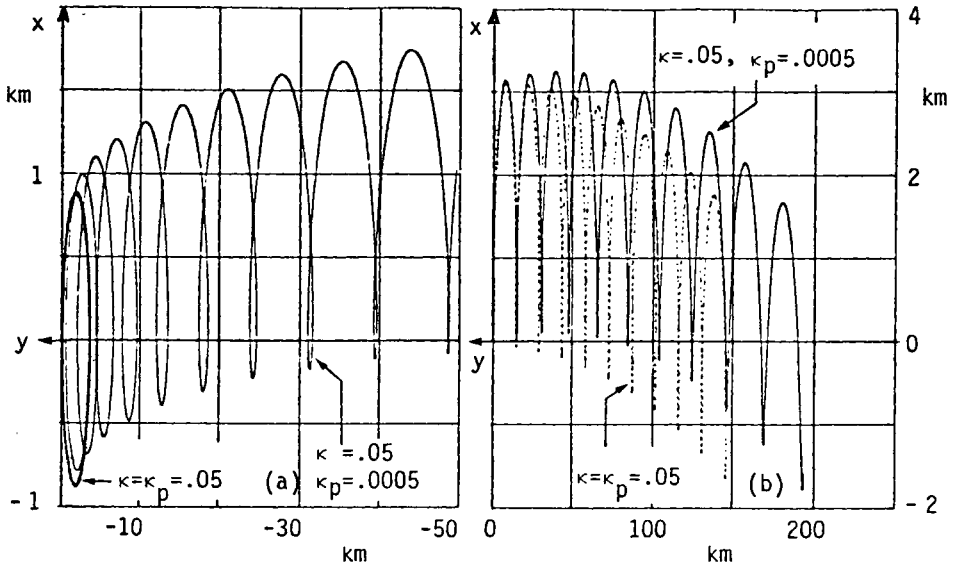

Fig. 4. Planar drag-perturbed relative trajectories for $\kappa \gg \kappa_p$. (a) $\Delta v = 1\,\mathrm{ms}^{-1}$, $\alpha = \beta = 0$; (b) $\Delta v = 1\,\mathrm{ms}^{-1}$, $\alpha = 60°$, $\beta = 0$.

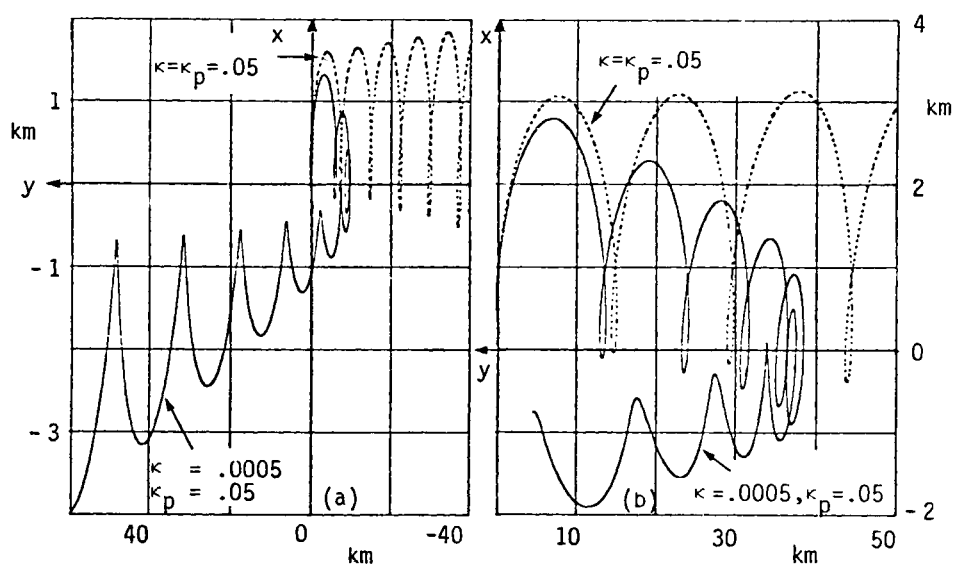

Fig. 5. Planar drag-perturbed relative trajectories for $\kappa \ll \kappa_p$. (a) $\Delta v = 0.5\,\mathrm{ms}^{-1}$, $\alpha = 120°$, $\beta = 0$ (b) $\Delta v = 0.85\,\mathrm{ms}^{-1}$, $\alpha = 90°$, $\beta = 0$.

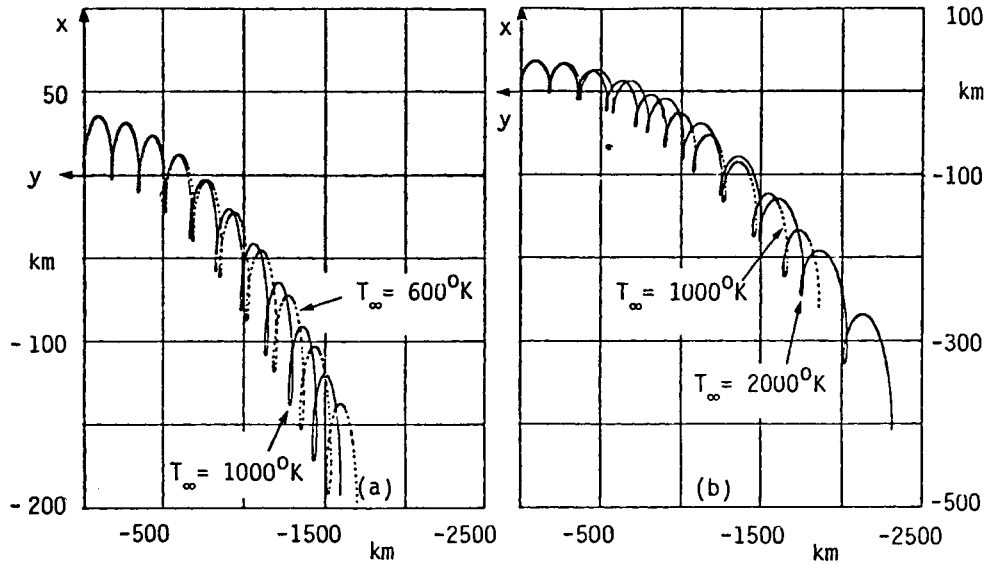

Fig. 6. Planar drag-perturbed relative trajectories, launched with $\Delta v = 10\,\mathrm{ms}^{-1}$, $\alpha = 90°$, $\beta = 0$, for different exospheric temperature. (a) $\kappa = 0.0005$, $\kappa_p = 0.05$; (b) $\kappa = 0.05$, $\kappa_p = 0.0005$.

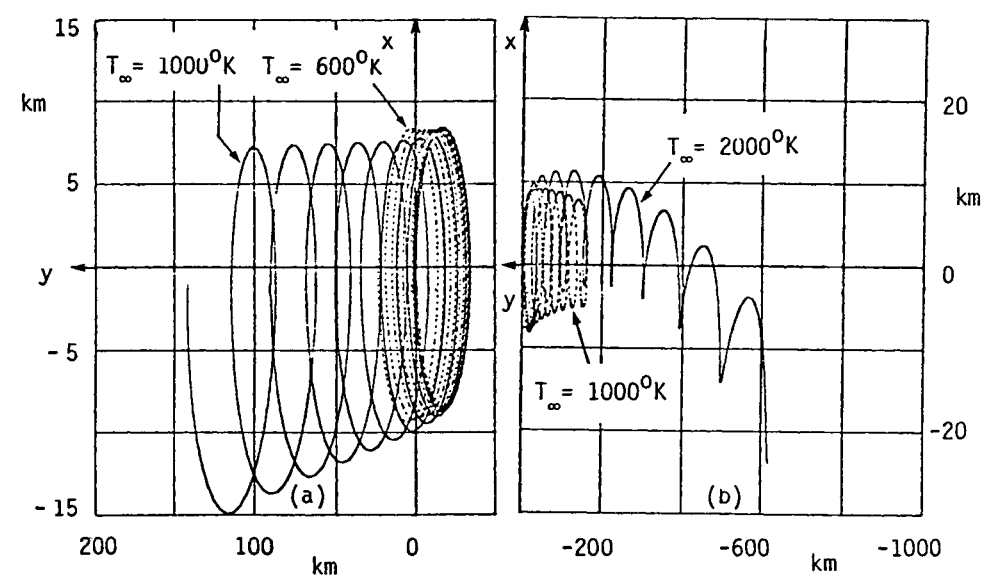

Fig. 7. Planar drag-perturbed relative trajectories, launched with $\Delta v = 10\,\mathrm{ms}^{-1}$, $\alpha = \beta = 0$, for different exospheric temperature. (a) $\kappa = 0.0005$, $\kappa_p = 0.05$ (b) $\kappa = 0.05$, $\kappa_p = 0.0005$.

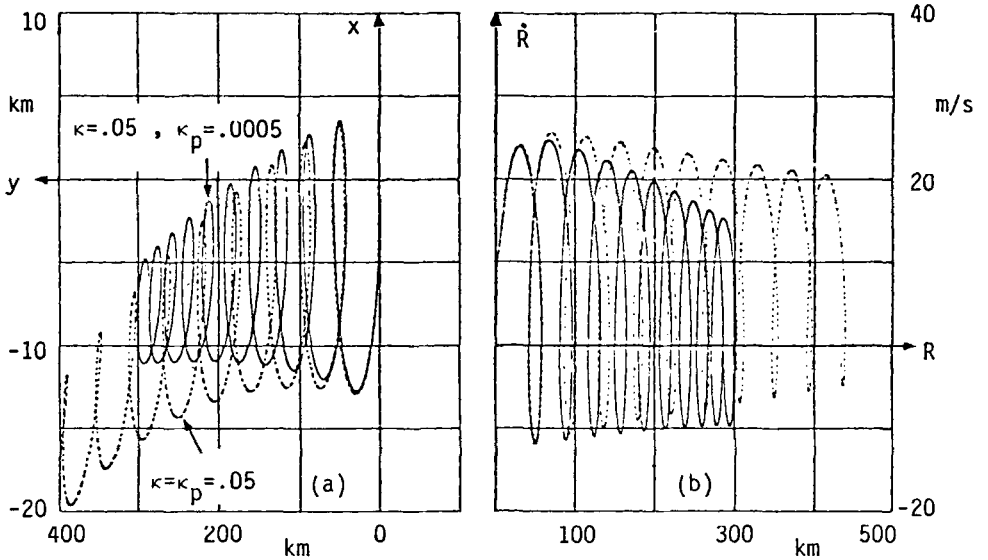

Fig. 8. Three-dimensional drag-perturbed relative trajectory, launched with $\Delta v = 10\ \mathrm{ms}^{-1}$, $\alpha = 150°$, $\beta = 120°$. (a) projected planar motion; (b) range vs range-rate.

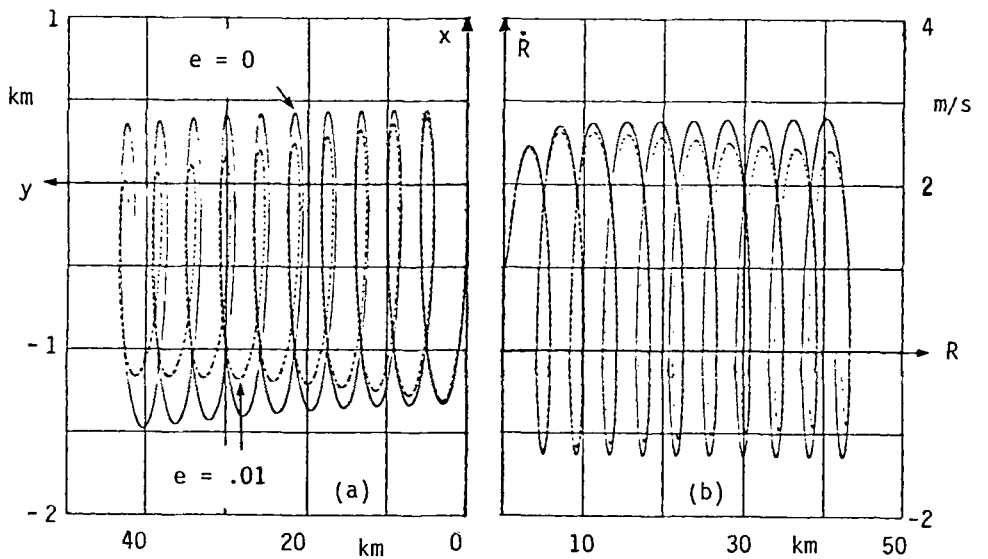

Fig. 9. Effect of station's eccentricity on three-dimensional relative trajectory, launched with $\Delta v = 1\ \mathrm{ms}^{-1}$, $\alpha = 150°$, $\beta = 120°$ and $\kappa = \kappa_p = 0.0005$. (a) projected planar motion; (b) range vs range-rate.

in Figures 6 and 7. The high temperature leads to a larger difference in energy loss than for the low T_∞ case. When $\kappa_p > \kappa$ the probe's energy surplus will be dissipated quicker for high T_∞ resulting in the faster angular rate than for low T_∞ as shown in Figure 6a. In the case $\kappa_p < \kappa$ the probe's mean angular rate at the high T_∞ will be less than that at the low temperature so that the probe lags further behind for high T_∞ as is illustrated in Figure 6b. The same qualitative effects are observed in Figures 7 where now the differences are more pronounced since the launch has not already introduced a difference in mean angular rate.

In Figure 8 a three-dimensional trajectory is shown in terms of its projected planar motion (a) and as a $(R, \dot{R})$ phase plane (b). For sufficiently small Δv the out-of-plane (z) motion can be considered as an harmonic oscillation with station's orbital period while the in-plane relative motion is similar to the planar trajectory obtained after a co-planar launch with the projected Δv. Thus, the same energy arguments as employed in the co-planar trajectories can be used here for obtaining a qualitative understanding of the resulting motion. In Figures 8 and 9 the probe is launched into a lower energy orbit. Due to its lower drag parameters the probe is regaining energy on the station in Figure 8 (solid curves). The influence of a small eccentricity in the station's orbit can be seen in Figure 9 where identical drag parameters for probe and station are taken. The discrepancy between the two patterns occurs predominantly in the x direction and is caused by the varying altitude of the station and the accompanying fluctations in density.

7. Concluding Remarks

A general three-dimensional theory for relative motion allowing the inclusion of arbitrary perturbing forces acting on both bodies has been presented and applied to air drag and Earth's oblateness perturbations. An exact analytical solution was found for the unperturbed case. It is important to note that the formulation in terms of relative elements allows considerable freedom in the choice of the perturbing forces. A more realistic air density model as the one used in the present paper can be accommodated by simply providing the time- and position-dependent force and difference force components.

Acknowledgement

The author acknowledges the award of an ESA Internal Fellowship. Special thanks go to Drs E. A. Roth and W. Flury for encouragement and discussions.

References

Brouwer, D. and Clemence, G. M.: 1961, *Methods of Celestial Mechanics*, Academic Press, New York.
Clohessy, W. H. and Wiltshire, R. S.: 1960, 'Terminal Guidance System for Satellite Rendez-vous', *J. Aerospace Sci.* **27**, 653, 674.

Duchoissois, G. and Dale, D.: 1975, AMPS-Subsatellite Study, Final Report, *Internal ESA Publication*, European Space Agency, Paris.
Fitzpatrick, P. M.: 1970, *Principles of Celestial Mechanics*, Academic Press, New York.
Jacchia, L. G.: 1977, Thermospheric Temperature, Density and Composition: New models, *SAO Special Report* No. 375, Smithsonian Astrophysical Observatory, Cambridge, Massachusetts.
Lancaster, E. R.: 1970, 'Relative motion of two particles in elliptic orbits', *AIAA J.* **8**, 1978.
Nacozy, P. and Szebehely, V.: 1976, 'The Computation of Relative Motion with Increased Precision, *Celest Mech* **13**, 449.
Stiefel, E. L. and Scheifele, G.: 1971, *Linear and Regular Celestial Mechanics*, Springer Verlag, Berlin.
Van der Ha, J. C. (1980): 'Exact Analytical Formulation of Planar Relative Motion', *Acta Astronautica* 7, 1.

Appendix I: Components of Matrices A and ΔA

The rotation matrix $A = [\alpha_{jk}]$ describes the transformation from the inertial unit vectors $\mathbf{U}_i$, $i = 1, 2, 3$, to the station's local unit vectors $\mathbf{u}_x, \mathbf{u}_y, \mathbf{u}_z$:

$$\begin{pmatrix} \mathbf{u}_x \\ \mathbf{u}_y \\ \mathbf{u}_z \end{pmatrix} = \begin{bmatrix} \alpha_{11} & \alpha_{12} & \alpha_{13} \\ \alpha_{21} & \alpha_{22} & \alpha_{23} \\ \alpha_{31} & \alpha_{32} & \alpha_{33} \end{bmatrix} \begin{pmatrix} \mathbf{U}_1 \\ \mathbf{U}_2 \\ \mathbf{U}_3 \end{pmatrix}, \tag{A1}$$

where the components α_{jk}, $j, k = 1, 2, 3$, depend on the instantaneous state of the station through the elements j, k, and L. The explicit dependence of α_{jk} on these elements can be derived from the corresponding classical expressions in terms of ω, Ω, and ϕ (e.g. Fitzpatrick 1970, Section 2.5):

$$\begin{aligned}
&\alpha_{13} = 2(j \sin L - k \cos L)/(1 + J), \\
&\alpha_{11} = k\alpha_{13} + \cos L, \quad \alpha_{12} = -j\alpha_{13} + \sin L, \\
&\alpha_{23} = 2(j \cos L + k \sin L)/(1 + J), \\
&\alpha_{21} = k\alpha_{23} - \sin L, \quad \alpha_{22} = -j\alpha_{23} + \cos L, \\
&\alpha_{31} = 2k/(1 + J), \quad \alpha_{32} = -2j/(1 + J), \quad \alpha_{33} = (1 - J)/(1 + J),
\end{aligned} \tag{A2}$$

where J is an abbreviation for $j^2 + k^2$. The elements of the inverse matrix A^{-1} follow immediately due to the orthogonality of A:

$$A^{-1} = A^T = [\alpha_{kj}], \quad j, k = 1, 2, 3. \tag{A3}$$

Similarly as in Equation (A1) one can describe the transformation between the probe's local x_p, y_p, z_p frame and the inertial frame. The elements of the rotation matrix A_p between $\mathbf{U}_j$ and $\mathbf{u}_{px}, \mathbf{u}_{py}, \mathbf{u}_{pz}$ can be designated as $(\alpha_p)_{jk}$. In accordance with our methodology for avoiding the loss of precision due to the subtraction of almost equal quantities the matrix A_p should not be employed directly but in the form $A + \Delta A$. The 'difference matrix' $\Delta A = [\Delta\alpha_{jk}]$ contains the projections of the

difference vectors $\Delta\mathbf{u}_x(=\mathbf{u}_{px}-\mathbf{u}_x)$, $\Delta\mathbf{u}_y$ and $\Delta\mathbf{u}_z$ upon the inertial X_1, X_2, X_3 axes:

$$\begin{pmatrix}\Delta\mathbf{u}_x\\ \Delta\mathbf{u}_y\\ \Delta\mathbf{u}_z\end{pmatrix}=\begin{bmatrix}\Delta\alpha_{11}\,\Delta\alpha_{12}\,\Delta\alpha_{13}\\ \Delta\alpha_{21}\,\Delta\alpha_{22}\,\Delta\alpha_{23}\\ \Delta\alpha_{31}\,\Delta\alpha_{32}\,\Delta\alpha_{33}\end{bmatrix}\begin{pmatrix}\mathbf{U}_1\\ \mathbf{U}_2\\ \mathbf{U}_3\end{pmatrix}. \tag{A4}$$

It should be emphasized that the matrix ΔA (in contrast with A) is *not* orthogonal. The components $[\Delta\alpha_{jk}]$ can be calculated from Equations. (A2) with full precision:

$$\begin{aligned}
\Delta\alpha_{13} &= 2[\Delta j\sin L-\Delta k\cos L+(j+\Delta j)\Delta(\sin L)-(k+\Delta k)\Delta(\cos L)-\\
&\quad-\alpha_{13}\Delta J/2]/K,\\
\Delta\alpha_{11} &= \Delta(\cos L)+(k+\Delta k)\Delta\alpha_{13}+\alpha_{13}\Delta k,\\
\Delta\alpha_{12} &= \Delta(\sin L)-(j+\Delta j)\Delta\alpha_{13}-\alpha_{13}\Delta j,\\
\Delta\alpha_{23} &= 2[\Delta j\cos L+\Delta k\sin L+(j+\Delta j)\Delta(\cos L)+(k+\Delta k)\Delta(\sin L)-\\
&\quad-\alpha_{23}\Delta J/2]/K,\\
\Delta\alpha_{21} &= -\Delta(\sin L)+(k+\Delta k)\Delta\alpha_{23}+\alpha_{23}\Delta k,\\
\Delta\alpha_{22} &= \Delta(\cos L)-(j+\Delta j)\Delta\alpha_{23}-\alpha_{23}\Delta j,\\
\Delta\alpha_{31} &= (2\Delta k-\alpha_{31}\Delta J)/K,\quad \Delta\alpha_{32}=-(2\Delta j+\alpha_{32}\Delta J)/K,\\
\Delta\alpha_{33} &= -2\Delta J/[K(1+J)],
\end{aligned}$$

with

$$\begin{aligned}
&\Delta J=(2j+\Delta j)\Delta j+(2k+\Delta k)\Delta k,\quad K=1+J+\Delta J,\\
&\Delta(\cos L)=-2\sin(\Delta L/2)\sin(L+\Delta L/2),\\
&\Delta(\sin L)=2\sin(\Delta L/2)\cos(L+\Delta L/2).
\end{aligned} \tag{A5}$$

It is seen that the components of the matrix ΔA depend on the three station's elements j, k, and L as well as the corresponding relative elements Δj, Δk, and ΔL.

Appendix II: Transformations between $(\mathbf{r}, \mathbf{v}; \Delta\mathbf{r}, \Delta\mathbf{v})$ and $(\mathbf{a}, \Delta\mathbf{a})$

First it is shown how the orbital elements $\mathbf{a}$ and the relative elements $\Delta\mathbf{a}$ can be calculated from the state vector $\mathbf{r}, \mathbf{v}; \Delta\mathbf{r}, \Delta\mathbf{v}$ with components in the inertial X_1, X_2, X_3 frame. Loss of precision is avoided at all stages:

$$\begin{aligned}
&h=|\mathbf{r}\times\mathbf{v}|;\\
&f=h^2/(\mu r)-1 \text{ with } r=|\mathbf{r}|;\\
&g=h\dot{r}/\mu,\quad \dot{r}=(\mathbf{r},\mathbf{v})/r;
\end{aligned}$$

$$\left.\begin{aligned} j &= -h_2/(h+h_3) \\ k &= h_1/(h+h_3) \end{aligned}\right\}, \quad h_j = (\mathbf{h}, \mathbf{U}_j), \quad j = 1, 2, 3:$$

$$L = \arctan\left[(r_2 + jr_3)/(r_1 - kr_3)\right], \quad r_j = (\mathbf{r}, \mathbf{U}_j), \quad j = 1, 2, 3;$$

$$\Delta h = (2\mathbf{h} + \Delta\mathbf{h}, \Delta\mathbf{h})/(h + h_p), \quad \Delta\mathbf{h} = (\mathbf{r} + \Delta\mathbf{r}) \times \Delta\mathbf{v} + \Delta\mathbf{r} \times \mathbf{v},$$

$$h_p = |(\mathbf{r} + \Delta\mathbf{r}) \times (\mathbf{v} + \Delta\mathbf{v})|;$$

$$\Delta f = \left[\Delta h(2h + \Delta h) - h^2\,\Delta r/r\right]/\left[\mu(r + \Delta r)\right],$$

$$\Delta r = (2\mathbf{r} + \Delta\mathbf{r}, \Delta\mathbf{r})/(r + r_p), \qquad r_p = |\mathbf{r} + \Delta\mathbf{r}|;$$

$$\Delta g = (h + \Delta h)\Delta(\dot{r})/\mu + g\Delta h/h,$$

$$\Delta(\dot{r}) = \left[(\mathbf{r}, \Delta\mathbf{v}) + (\Delta\mathbf{r}, \mathbf{v} + \Delta\mathbf{v}) - \dot{r}\Delta r\right]/(r + \Delta r);$$

$$\left.\begin{aligned} \Delta j &= \left[h_2(\Delta h + \Delta h_3)/(h + h_3) - \Delta h_2\right]/(h + h_3 + \Delta h + \Delta h_3) \\ \Delta k &= -\left[h_1(\Delta h + \Delta h_3)/(h + h_3) - \Delta h_1\right]/(h + h_3 + \Delta h + \Delta h_3) \end{aligned}\right\},$$

$$\Delta h_j = (\Delta\mathbf{h}, \mathbf{U}_j), \quad j = 1, 2, 3;$$

$$\Delta L = \arctan\left[(D\Delta N - N\Delta D)/(D^2 + N^2 + D\Delta D + N\Delta N)\right],$$

$$N = r_2 + jr_3, \quad D = r_1 - kr_3, \quad \Delta N = \Delta r_2 + \Delta(jr_3),$$

$$\Delta D = \Delta r_1 - \Delta(kr_3). \tag{A6}$$

One should be aware of the following notational convention for differences in vector lengths: for instance, Δr stands for $\Delta|\mathbf{r}| = |\mathbf{r} + \Delta\mathbf{r}| - |\mathbf{r}|$ and is in general different from $|\Delta\mathbf{r}|$.

Next the converse relationships expressing the vectors $(\mathbf{r}, \mathbf{v}, \Delta\mathbf{r}, \Delta\mathbf{v})$ in terms of the elements $(\mathbf{a}, \Delta\mathbf{a})$ are derived. The orbital distance r, the radial velocity component $\dot{r}$ as well as their corresponding difference quantities Δr and $\Delta(\dot{r})$ will play an important role in these expressions. These four variables can readily be written in terms of elements and relative elements:

$$r = h^2/\left[\mu(1 + f)\right]; \quad \dot{r} = \mu g/h;$$

$$\Delta r = \left[(2h + \Delta h)\Delta h - h^2\Delta f/(1 + f)\right]/\left[\mu(1 + f + \Delta f)\right];$$

$$\Delta(\dot{r}) = \mu\Delta(g/h) = \mu\left[\Delta g - g\Delta h/h\right]/(h + \Delta h). \tag{A7}$$

The inertial components of the vectors $\mathbf{r}$ and $\mathbf{v}$ follow from $\mathbf{r} = r\mathbf{u}_x$ and $\mathbf{v} = \dot{r}\mathbf{u}_x + (h/r)\mathbf{u}_y$, Equations (8), after performing the coordinate transformation of Equations (A1):

$$r_j = (\mathbf{r}, \mathbf{U}_j) = r\alpha_{1j}, \quad v_j = (\mathbf{v}, \mathbf{U}_j) = \dot{r}\alpha_{1j} + (h/r)\alpha_{2j}, \quad j = 1, 2, 3. \tag{A8}$$

The difference vectors $\Delta\mathbf{r}$ and $\Delta\mathbf{v}$ can be written in the full precision forms:

$$\Delta\mathbf{r} = r\Delta\mathbf{u}_x + \Delta r(\mathbf{u}_x + \Delta\mathbf{u}_x),$$

$$\Delta\mathbf{v} = \dot{r}\Delta\mathbf{u}_x + \Delta(\dot{r})(\mathbf{u}_x + \Delta\mathbf{u}_x) + (h/r)\Delta\mathbf{u}_y + \Delta(h/r)(\mathbf{u}_y + \Delta\mathbf{u}_y). \tag{A9}$$

Expanding the local unit-vectors and difference-unit-vectors in terms of their projections on the inertial reference axes, i.e. the components of the matrices of Equations (A1) and (A4), one obtains:

$$\Delta r_j = (\Delta\mathbf{r}, \mathbf{U}_j) = r\Delta\alpha_{1j} + (\alpha_{1j} + \Delta\alpha_{1j})\Delta r,$$

$$\Delta v_j = (\Delta\mathbf{v}, \mathbf{U}_j) = \dot{r}\Delta\alpha_{1j} + (\alpha_{1j} + \Delta\alpha_{1j})\Delta(\dot{r}) + (h/r)\Delta\alpha_{2j} + (\alpha_{2j} + \Delta\alpha_{2j})\Delta(h/r),$$

$$j = 1, 2, 3. \tag{A10}$$